Macromolecules

pubs.acs.org/Macromolecules

Article

Detergent-Free Functionalization of Hybrid Vesicles with Membrane Proteins Using SMALPs

Rosa Catania, Jonathan Machin, Michael Rappolt, Stephen P. Muench, Paul A. Beales,* and Lars J. C. Jeuken*

Cite This: https://doi.org/10.1021/acs.macromol.2c00326

Read Online

ACCESS | Metrics & More | Article Recommendations | Supporting Information

ABSTRACT: Hybrid vesicles (HVs) that consist of mixtures of block copolymers and lipids are robust biomimetics of liposomes, providing a valuable building block in bionanotechnology, catalysis, and synthetic biology. However, functionalization of HVs with membrane proteins remains laborious and expensive, creating a significant current challenge in the field. Here, using a new approach of extraction with styrene-maleic acid (SMA), we show that a membrane protein (cytochrome bo_3) directly transfers into HVs with an efficiency of 73.9 ± 13.5% without the requirement of detergent, long incubation times, or mechanical disruption. Direct transfer of membrane proteins using this approach was not possible into liposomes, suggesting that HVs are more amenable than liposomes to membrane protein incorporation from a SMA lipid particle system. Finally, we show that this transfer method is not limited to cytochrome bo_3 and can also be performed with complex membrane protein mixtures.

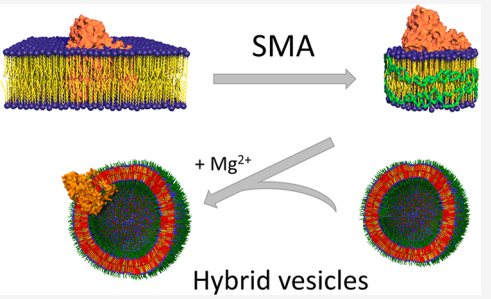

INTRODUCTION

Vesicles made of natural or synthetic lipids (liposomes) are a suitable platform for mimicking membrane structures and functions found in nature.[1,2] Liposomes have been widely exploited to fabricate artificial compartments in bottom-up synthetic biology (artificial cells and organelles) and nanoreactors in compartmentalized (photo)catalysis.[3,4] Functionalization of liposomes in biotechnology is achieved by the reconstitution of membrane proteins (MPs), which in spite of their complex amphiphilic nature, have an increasing number of promising applications in areas such as drug discovery,[5] vaccines,[6] biosensors,[7] and energy conversion.[8] However, the application of proteoliposomes is still hampered by the lack of chemical and physical long-term stability (typically days)[9] and the complexity of purification and reconstitution of MPs.[10,11]

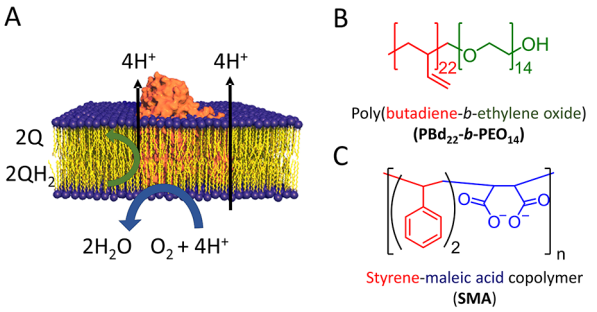

Figure 1. (A) Schematic representation of the structure and function of cyt bo_3 (orange) embedded in the lipid bilayer (represented with yellow lipid tails and blue head groups). (B) Chemical structures of PBd_{22}-*b*-PEO_{14} copolymer, with the polybutadiene block polymer in red and the polyethylene glycol block polymer in green. (C) SMA (2:1) copolymer, with the styrene group in red and the maleic acid group in blue.

Recent developments using amphiphilic polymers have shown promise in solving these experimental limitations. Amphiphilic polymers can self-assemble into robust and stable vesicles, known as polymersomes.[12,13] Despite the advantageous stability and tunability of these synthetic vesicles,[14] the non-native polymeric environment can limit the functional incorporation of many MPs.[15] Hybrid vesicles (HVs), composed of a mixture of block copolymers and lipids, have proven to be a balanced compromise between liposome biocompatibility and polymersome stability.[16−20] Several block copolymers have been studied to correlate how their chemical structure affects the overall properties of the HVs, and both well-mixed and phase-separated membranes have been used.[15,21,22] We have previously shown that the membrane protein cytochrome bo_3 (cyt bo_3) can be functionally reconstituted into HVs containing up to 50 mol % of the diblock copolymer poly(butadiene-*b*-ethylene oxide) (PBd_{22}-*b*-PEO_{14}) with POPC lipids, with minimal loss in protein activity and enhanced lifetime up to 500 days.[16,23]

Received: February 14, 2022
Revised: April 8, 2022

Despite the promise of polymersomes and HVs, the process of extraction, purification, and functional reconstitution of MPs still presents major challenges. Reconstitution methods into polymersomes and HVs are based on methods developed for reconstitution in liposomes, which require detergents and often extensive optimization. Detergents can destabilize MPs by inducing protein unfolding, dissociation of small subunits, and removal of natural lipids associated with the protein hydrophobic regions, and consequently compromise their activity and limit their functional lifetime.[24−26] Thus, the selection of a compatible detergent and optimum condition to extract a target protein can be a laborious, time-consuming, and risk-prone procedure.[27,28]

Here, we report a novel strategy for the reconstitution of a membrane protein, cyt bo_3, from *Escherichia coli* (Figure 1A), into HVs. Cyt bo_3 is a four-subunit membrane enzyme complex (~143 kDa) from *E. coli* that belongs to the heme-copper oxidase enzyme family and, as such, accepts electrons from ubiquinol and passes them onto molecular oxygen, coupling the electron transfer with proton pumping across the membrane (Figure 1A).[29] Activity of cyt bo_3, and thus functional reconstitution into the membrane vesicles, is commonly evaluated by measuring oxygen consumption. For the HVs, we selected PBd_{22}-*b*-PEO_{14} (MW 1.8 kDa) (Figure 1B), as this copolymer is a compromise between the stability of higher MW polymers and minimizing the difference in hydrophobic thickness between the membranes of pure polymer and pure lipid systems and forms a homogeneous blend with lipids.[15,30]

Using a novel procedure, we show that reconstitution of cyt bo_3 into HVs does not require the use of a detergent. Instead, insertion of cyt bo_3 into the HVs is accomplished by a second amphiphilic polymer, styrene-maleic acid copolymer (SMA, Figure 1C). SMA and similar polymers have emerged as an effective material to extract and solubilize MPs, including cyt bo_3,[31] while preserving protein activity,[32] overcoming issues encountered with detergent-mediated solubilization.[33,34] SMA is an anionic copolymer containing carboxylic acid pendant groups in the form of maleic acid alternating with the hydrophobic styrene pendant groups (Figure 1C).

Unlike detergents, SMA copolymers do not self-assemble into micelles.[35] When added to cellular membrane extracts, the hydrophobic styrene groups of SMA copolymers intercalate between the acyl chains of the lipid bilayer, whereas the hydrophilic maleic acid groups interface with the solvent.[32] This interaction between SMA copolymers and membranes leads to the spontaneous formation of discoidal particles of ~10 nm diameter.[36] SMA copolymers offer the advantage of solubilizing MPs directly from the cell membrane by forming these nanodisc structures, called SMA−lipid particles (SMALPs), which retain the natural lipids associated with the MPs.[37,38] MPs can be purified from SMALPs by affinity chromatography.[39] Besides their use for structural and functional studies,[39] SMALPs have recently been shown to mediate reconstitution of MPs into planar lipid bilayers, as the tetrameric K^+ channel,[40] and into liposomes, as exemplified for a cytochrome *c* oxidase[41] and a Na^+/H^+ antiporter.[42] In addition to SMA, other maleic acid copolymers capable of solubilizing MPs have been synthesized with various chemical functionalities, such as aliphatic side chains replacing the styrene group[43−45] or differently charged moieties in the maleic group, providing a diverse toolkit of potential polymers.[45−47]

RESULTS

First, we investigated the stability of HVs when exposed to increasing concentrations of SMA copolymer (Figures S2 and S3). SMA is seen to solubilize HVs at an SMA to lipid and PBd_{22}-*b*-PEO_{14} copolymer ratio of 1 (mol_{SMA}/$mol_{(Lipids+PBd22\text{-}b\text{-}PEO14)}$), with less SMA needed to solubilize HVs than liposomes. Still, the amount of SMA required to

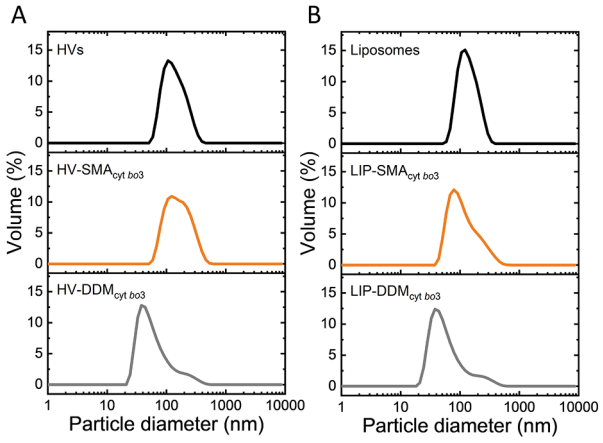

Figure 2. Physical characterization of membrane vesicles. Dynamic light scattering (DLS) volume profiles of (A) HVs, HV-$SMA_{cyt\ bo3}$, and HV-$DDM_{cyt\ bo3}$ and (B) liposomes, LIP-$SMA_{cyt\ bo3}$, and LIP-$DDM_{cyt\ bo3}$. The concentration of analyzed samples was 0.5 mg/mL of total PBd_{22}-*b*-PEO_{14} polymer and lipid components.

Table 1. Reconstitution Efficiency of $SMA_{cyt\ bo3}$ and $DDM_{cyt\ bo3}$ in Vesicles As Quantified by UV−Vis Spectroscopy of the Soret Band (409 nm)

vesicle sample	reconstitution efficiency (%)	±SD
HV-$SMA_{cyt\ bo3}$	73.9	±13.5
LIP-$SMA_{cyt\ bo3}$	not detected	
HV-$DDM_{cyt\ bo3}$	61.0	±7.5
LIP-$DDM_{cyt\ bo3}$	58.0	±3.5

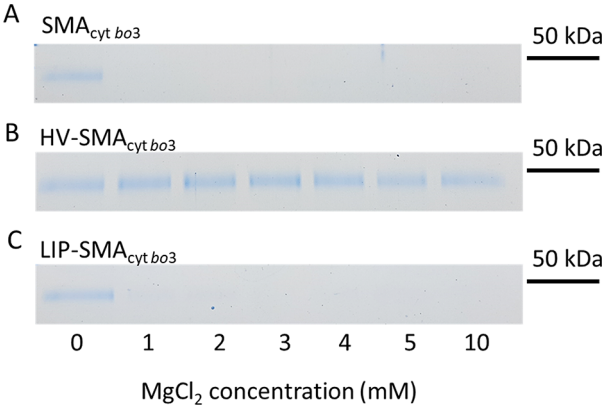

Figure 3. Analysis of (A) $SMA_{cyt\ bo3}$, (B) HV-$SMA_{cyt\ bo3}$, and (C) LIP-$SMA_{cyt\ bo3}$. After direct incubation of $SMA_{cyt\ bo3}$ with HVs or liposomes, samples were incubated with increasing Mg^{2+} concentration for 2 h, followed by centrifugation at 17000*g* for 15 min to pellet nonreconstituted $SMA_{cyt\ bo3}$. The supernatant containing HVs or liposomes was analyzed with SDS-PAGE (Coomassie Blue staining). Only subunit I of cyt bo_3 is shown. The entire gel is shown in Figure S5.

https://doi.org/10.1021/acs.macromol.2c00326
Macromolecules XXXX, XXX, XXX−XXX

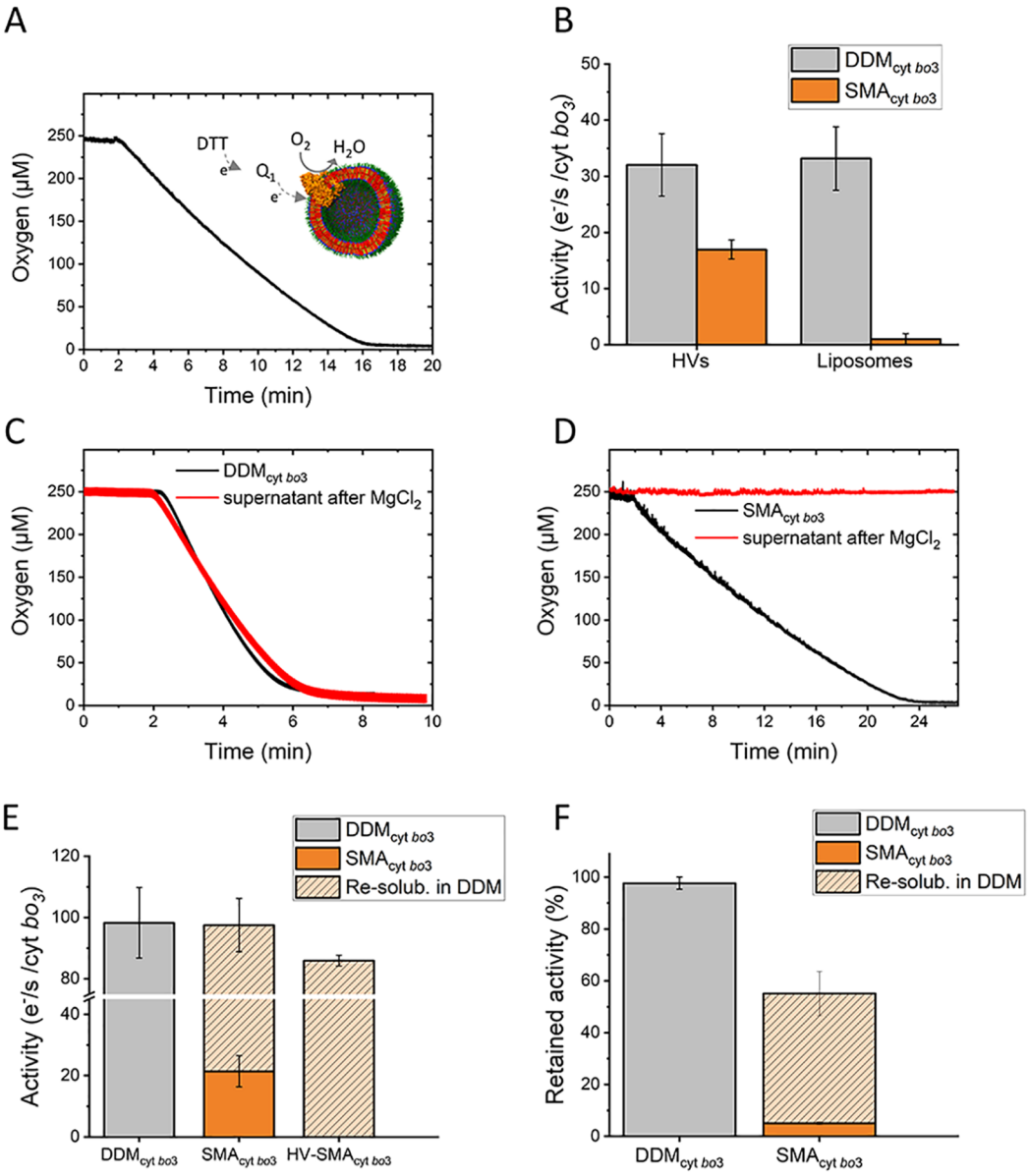

Figure 4. (A) Oxygen consumption trace for HV-$SMA_{cyt\ bo3}$. The oxygen consumption rate was determined via regression of the first 30 s from the slope and normalized by the protein concentration. (B) Comparison of the activities of reconstituted cyt bo_3 determined via oxygen consumption. Error bars represent the standard deviation of three independent experiments. (C) Oxygen consumption traces for $DDM_{cyt\ bo3}$ and (D) $SMA_{cyt\ bo3}$. The traces show the activity before and after $MgCl_2$ treatment. (E) Comparison of the activities of soluble $SMA_{cyt\ bo3}$ and $DDM_{cyt\ bo3}$ determined via oxygen consumption. The graph also shows the activity of soluble $SMA_{cyt\ bo3}$ and HV-$SMA_{cyt\ bo3}$ after resolubilization in DDM (1%). Error bars represent the standard deviation of three independent experiments. (F) Activity retention after incubation with 10 mM $MgCl_2$ and centrifugation for the supernatant fractions of soluble $DDM_{cyt\ bo3}$, soluble $SMA_{cyt\ bo3}$, and soluble $SMA_{cyt\ bo3}$ in the presence of 1% DDM. The activity retention was determined via comparison of the oxygen consumption rate (determined via regression of the first 30 s from the slope and normalized by the protein concentration) before and after $MgCl_2$ treatment and centrifugation.

reconstitute cyt bo_3 is about 20 time less (see below), and thus we excluded that the presence of SMA during the reconstitution of cyt bo_3 could affect the stability of the hybrid vesicles.

SMA-solubilized cyt bo_3 ($SMA_{cyt\ bo3}$) were prepared from membrane extracts of *E. coli* GO105/pJRhisA[48] (protein content ~4 mg/mL), containing His-tagged cyt bo_3, by incubation with 2% (w/v) SMA for 2 h at room temperature (RT) and purified via Ni-NTA affinity chromatography (as described in the Supporting Information). Purity of $SMA_{cyt\ bo3}$ was confirmed in a direct comparison with a previous published procedure[48] using *n*-dodecyl-*β*-D-maltoside (Figure S1, $DDM_{cyt\ bo3}$).

$SMA_{cyt\ bo3}$ and $DDM_{cyt\ bo3}$ were reconstituted into HVs and lipid-only liposomes (*E. coli* "polar" lipid extract, LIP). As such, four vesicle samples are compared, which hereafter will be named (1) HV-$SMA_{cyt\ bo3}$, (2) HV-$DDM_{cyt\ bo3}$, (3) LIP-$SMA_{cyt\ bo3}$ and (4) LIP-$DDM_{cyt\ bo3}$. HVs were composed of PBd_{22}-*b*-PEO_{14} and *E. coli* "polar" lipid extracts at a 1:1 mol/mol ratio.

Reconstitution of $DDM_{cyt\ bo3}$ into HV-$DDM_{cyt\ bo3}$ and LIP-$DDM_{cyt\ bo3}$ was performed by destabilization with detergent

https://doi.org/10.1021/acs.macromol.2c00326
Macromolecules XXXX, XXX, XXX−XXX

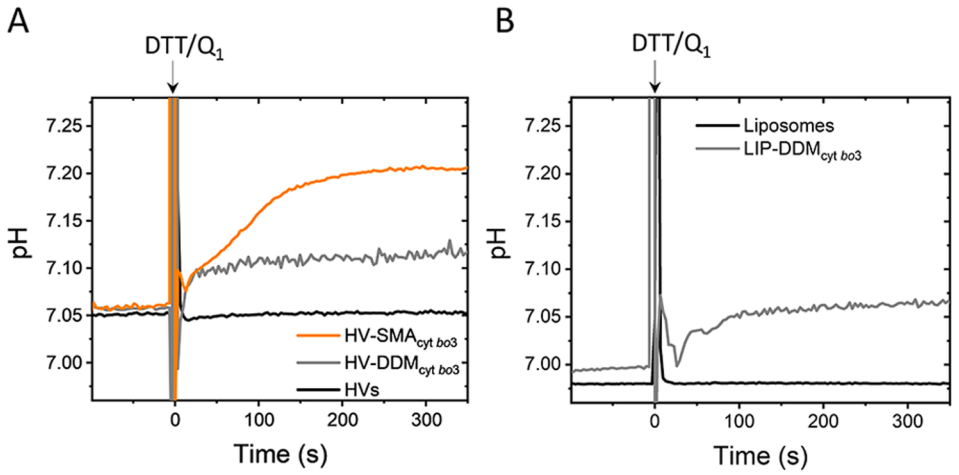

Figure 5. Intravesicular pH change for (A) HVs, HV-SMA$_{cyt\ bo3}$, and HV-DDM$_{cyt\ bo3}$ and (B) liposomes and LIP-DDM$_{cyt\ bo3}$. Displayed curves are representatives of three independent experiments.

Table 2. Solubilization Efficiency of *E. coli* Membrane Protein Extract *via* SMALPs and subsequent reconstitution efficiency into HVs[a]

	SMALP fraction	solubilization efficiency (%)	±SD
before $MgCl_2$ addition	total	52.6	4.6
after $MgCl_2$ and centrifugation	supernatant	<1	<1
	pellet	43.5	8.6
before $MgCl_2$ addition	HVs	53.1	2.2
after $MgCl_2$ and centrifugation	HVs (supernatant)	29.4	6.8
	HVs (pellet)	21.6	5.3

[a]Solubilization efficiency was determined by BCA assay and expressed as a percentage of total MP content prior to SMA solubilization.

(Triton X-100), followed by extensive removal of the detergent by Biobeads, as previously reported[16] (described in the Supporting Information). To reconstitute SMA$_{cyt\ bo3}$, we took advantage of SMA precipitating in the presence of $MgCl_2$ (>5 mM) due to the interactions of the divalent cation Mg^{2+} with the maleic acid groups.[49] Without the SMA belt, the lipid particles become unstable and will precipitate with the contained MP, unless reconstituted. This strategy has previously been used to exchange the membrane protein AcrB from SMALP into an amphipol scaffold.[38] SMA$_{cyt\ bo3}$ was incubated with HVs (or liposomes as control) on ice for 30 min at a protein to lipid ratio of ∼1:100 (w/w) and then incubated with 10 mM $MgCl_2$ to precipitate SMA. Cyt bo_3 that was not reconstituted into HVs or liposomes was removed by centrifugation at 17000*g* for 15 min. Treatment with 10 mM $MgCl_2$ does not affect the size of the vesicles (Figure S4).

Dynamic light scattering (DLS) analysis of the four reconstituted samples in Figure 2 (see Table S1 for details) showed that the diameter of the HVs (Figure 2A) slightly increased after SMA$_{cyt\ bo3}$ reconstitution (from ∼130 nm to ∼150 nm), but otherwise remain largely unaltered. In contrast, DDM$_{cyt\ bo3}$ reconstitution into HV shows a clear reduction in liposome size and an increase in polydispersity (see Table S1). The same is observed for the reconstitution of DDM$_{cyt\ bo3}$ in liposomes (Figure 2B). The decreases in size suggest that the Biobead treatment might extract lipids from the HVs and liposomes. The reason for the increase in polydispersity during the DDM reconstitution is unknown, but we hypothesize that some cyt bo_3 might not properly have reconstituted, causing some aggregation in the sample.

The reconstitution efficiency of cyt bo_3 was quantified by solubilization of the vesicles with Triton X-100 and UV analysis of the Soret peak of cyt bo_3 (409 nm). Interestingly, the reconstitution efficiency of SMA$_{cyt bo3}$ was profoundly different between HVs and liposomes (Table 1). SMA$_{cyt\ bo3}$ could be directly reconstituted into HVs but not into liposomes. This difference in reconstitution efficiency between HVs and liposomes was also confirmed by sodium dodecyl sulfate polyacrylamide gel electrophoresis (SDS-PAGE) (Figure 3 and Figure S5).

The activities of reconstituted cyt bo_3 were compared by measuring the rates of oxygen consumption with the substrate ubiquinol 1 (Q_1) (200 μM), which is reduced by dithiothreitol (DTT) (2 mM) (Figure 4A, see Supporting Information for details). Figure 4B shows the activity of SMA$_{cyt\ bo3}$ after reconstitution into either HVs or liposomes. In correspondence with the results above, LIP-SMA$_{cyt\ bo3}$ did not exhibit any substantial enzyme activity, in line with the fact that SMA$_{cyt\ bo3}$ does not reconstitute into liposomes. In contrast, HV-SMA$_{cyt\ bo3}$ shows clear activity, about half that of the control samples HV-DDM$_{cyt\ bo3}$ and LIP-DDM$_{cyt\ bo3}$ (Figure 4B). We note that, before reconstitution, the activity of the soluble SMA$_{cyt\ bo3}$ is significantly lower than the activity of DDM$_{cyt\ bo3}$ (Figure 4C−E). A reduction in activity has been previously reported for other enzymes in SMALPs.[50,51] The same reduction in activity is also apparent after DDM$_{cyt\ bo3}$ is reconstituted into liposomes (LIP-DDM$_{cyt\ bo3}$). We speculate that this might be an experimental artifact due to differences in substrate access (Q_1) to the quinol-binding site of the enzyme in DDM micelles vs the enzyme embedded into lipid membranes or SMALPs. Importantly, after resolubilization in 1% DDM detergent of both soluble SMA$_{cyt\ bo3}$ and HV-SMA$_{cyt\ bo3}$, cyt bo_3 regains an activity similar to DDM$_{cyt\ bo3}$ (Figure 4E and F). This confirms that neither the solubilization of cyt bo_3 into SMALPs nor the reconstitution into HVs irreversibly changes cyt bo_3 and supports our hypothesis that the reduction in activity is due to the enzyme assay which utilizes a non-natural substrate analogue, Q_1. This is further supported by a structure of cyt bo_3 that was shown not to be affected by solubilization with a slightly different SMA copolymer (3:1).[31]

https://doi.org/10.1021/acs.macromol.2c00326
Macromolecules XXXX, XXX, XXX−XXX

In order to confirm that reconstituted cyt bo_3 was fully inserted across the membranes of HVs, we evaluated the net change in intravesicular pH due to the proton-pumping activity of the enzyme upon chemical activation. Changes in internal pH were determined by ratiometric fluorescence measurements of the pH-sensitive fluorescent probe 8-hydroxypyrene-1,3,6-trisulfonic acid (HPTS) (Figure S6, see Supporting Information for details). While HVs showed a constant intravesicular pH after the addition of DTT and Q_1, both HV-$SMA_{cyt\ bo3}$ and HV-$DDM_{cyt\ bo3}$ displayed an increase of intravesicular pH (Figure 5A), similarly to LIP-$DDM_{cyt\ bo3}$ (Figure 5B). The increase in pH indicates that the cyt bo_3 was successfully inserted into the membrane with a prevalence of an "outward" orientation, as previously demonstrated in liposomal reconstitution.[52,53]

To further assess the ability of SMA to facilitate the reconstitution of membrane proteins (MPs) into HVs, we attempted the reconstitution of the full MPs composition of *E. coli*. To do this, an *E. coli* membrane extract (GO105/pJRhisA) was solubilized with SMA and nonsolubilized material removed by ultracentrifugation (100000*g* for 60 min). This full extract of all SMALPs was incubated with HVs on ice for 30 min, at a 2:8 protein mass to polymer and lipids mass ratio. MPs not reconstituted into HVs were again precipitated by addition of 10 mM $MgCl_2$ and removed by centrifugation (17000*g* for 15 min). We compared the protein solubilization efficiencies of soluble and reconstituted MPs by measuring the protein concentration (bicinchoninic acid (BCA) assay, Table 2). Overall, 52.6 (±4.6)% of the *E. coli* MPs were solubilized by SMA. After reconstitution, more than half of this fraction (29.4 (±6.8)%) was successfully reconstituted into HVs.

To assess whether the protein content after reconstitution into HVs was a true representation of the various MPs from native membranes of *E. coli*, we conducted an SDS-PAGE analysis for qualitative comparison (Figure 6A). SDS-PAGE showed very similar profiles for each condition, strongly suggesting that SMA can extract a wide range of membrane proteins and transfer these to HVs. This analysis also confirmed that precipitation of SMALPs with 10 mM $MgCl_2$ (i.e., without HVs) removed the entire protein content if not reconstituted. Finally, we evaluated whether the MPs were functionally active after reconstituted into HVs by monitoring the activity of the cyt bo_3, which was part of the MP extract mixture. Figure 6B and Figure S7 show the oxygen reduction activity of the full MP extracts solubilized by SMA before (SMA_{MPs}) and after (HV-SMA_{MPs}) reconstitution into HVs. The activity confirms that cyt bo_3 was functionally active after transfer into HVs, indicating that complex mixtures of proteins can be reconstituted with SMA. The oxygen reduction activity, normalized against total MP content, is lower after reconstitution in HVs, and we hypothesize that this is due to different efficiencies of reconstitution of the various MPs.

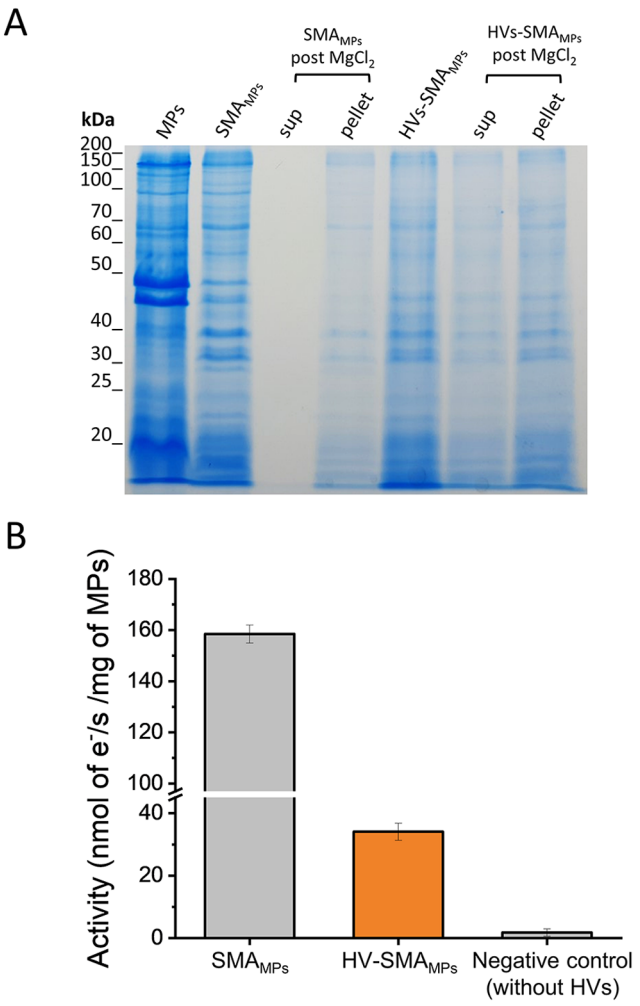

Figure 6. (A) SDS-PAGE (15%) analysis of membrane protein samples contained in either SMA_{MPs} or HV-SMA_{MPs} before and after treatment with $MgCl_2$ and separation of the insoluble part via precipitation. The concentration of *E. coli* membrane-protein fraction (MPs, lane 1) was halved in comparison to the other loaded samples to improve the quality of the SDS-PAGE. (B) Comparison of the oxygen-reducing activities of soluble SMA_{MPs}, HV-SMA_{MPs}, and SMA_{MPs} treated with $MgCl_2$ without HVs ("negative control"). The activity is normalized per mg of total MP content for SMA_{MPs} and HV-SMA_{MPs} determined via BCA assay. Error bars represent the standard deviation of three independent experiments.

DISCUSSION AND CONCLUSIONS

Although SMA-solubilized proteins have previously been shown to reconstitute into planar lipid bilayers[40] or liposomes,[41,42] the mechanisms by which this happens is not fully understood. Indeed, little is known about the interaction between SMALPs and lipid membranes, although it has been shown that the lipid packing properties and electrostatic interactions strongly influence how SMA interplays with the lipid bilayer.[54] Particularly, phospholipid phosphoethanolamine (PE), characterized by a negative intrinsic curvature,[55] exerts a lateral pressure that hampers SMA insertion and, therefore, membrane solubilization.[54,56,57] Similarly, we hypothesize that PE might hamper SMA reconstitution of MPs back into liposomes. This may explain the lack of reconstitution of $SMA_{cyt\ bo3}$ into the liposomes in this study, which were prepared from an *E. coli* "polar" lipid extract (PE, ~65 mol %; PG, ~25 mol %; and cardiolipin, ~10 mol %).[15]

We have previously observed that hybrid giant unilamellar vesicles (GUVs) of PBd_{22}-*b*-PEO_{14} and 1-palmitoyl-2-oleoyl-sn-glycero-3-phosphocholine (POPC) are well-mixed and homogeneous with a similar molecular ordering and packing, but lower fluidity, than POPC lipid bilayers.[58] Previous works have also shown that the area stretching moduli (K_a) of polymersomes made of PBd-*b*-PEO polymers (90−130 mN/m[59,60]) are much lower than the typical K_a for phosphocholine liposomes (200−260 mN/m).[60,61] For HVs composed of PBd_{22}-*b*-PEO_{14} and 1,2-Dioleoyl-sn-glycero-3-phosphocholine

https://doi.org/10.1021/acs.macromol.2c00326
Macromolecules XXXX, XXX, XXX−XXX

(DOPC), or PBd_{46}-*b*-PEO_{30} mixed with POPC, the area stretching modulus lies intermediate between that of pure polymer and pure lipid vesicles.[18,60] While comparable data are not available for mixtures of *E. coli* polar lipid extract and PBd_{22}-*b*-PEO_{14}, we infer that the block copolymer will impart a similar reduction in the stretching modulus of vesicles in this work. Importantly, the area stretching modulus is proportional to the surface tension (γ) of the membrane ($K_a \sim 4\gamma$). The decreased surface tension and reduced work required to stretch the interface likely reduce the energy barrier for the transfer of cyt bo_3 from the SMALPs to the HV membrane. It has previously been hypothesized that this enhanced elasticity of hybrid PBd_{22}-*b*-PEO_{14} membranes lowers the energy cost for membrane deformations required to accommodate insertion of the membrane protein.[18] Thus, here, we consider the higher elasticity of the HV compared to liposomes to be essential for reconstitution of MPs from SMALPs.

In conclusion, we show for the first time the reconstitution of SMA-solubilized membrane protein either as pure isolated protein ($SMA_{cyt\ bo3}$) or as a complex MP mixture (SMA_{MPs}), into vesicles without the use of detergents while maintaining protein activity. For cytochrome *c* oxidase, sonication or extrusion was required to induce its reconstitution into liposomes,[41] while for plasma membrane Na^+/H^+ antiporter, a much longer incubation time (overnight) with liposomes of larger diameter (400 nm) was needed and only ~10% reconstitution was achieved.[42] In contrast, a simple incubation for 30 min on ice is sufficient to reconstitute $SMA_{cyt\ bo3}$ into HVs, while the same procedure does not lead to a transfer of cyt bo_3 to liposomes. This method provides a new tool to reduce time and cost for enzyme reconstitution processes by avoiding detergent-mediated reconstitution and represents a solid foundation for further development as an enabling technology for MPs in nanomedicine, biocatalysis, and bottom-up synthetic biology.

■ ASSOCIATED CONTENT

Supporting Information

The Supporting Information is available free of charge at https://pubs.acs.org/doi/10.1021/acs.macromol.2c00326.

Experimental procedures, SDS-PAGE analyses, destabilization profiles, and additional oxygen consumption traces (PDF)

■ AUTHOR INFORMATION

Corresponding Authors

Paul A. Beales − *Astbury Centre of Structural Molecular Biology and School of Chemistry, University of Leeds, Leeds LS2 9JT, U.K.;* orcid.org/0000-0001-9076-9793; Email: P.A.Beales@leeds.ac.uk

Lars J. C. Jeuken − *Astbury Centre of Structural Molecular Biology and School of Biomedical Sciences, University of Leeds, Leeds LS2 9JT, U.K.; Leiden Institute of Chemistry, University Leiden, Leiden 2300RA, The Netherlands;* orcid.org/0000-0001-7810-3964; Email: L.J.C.Jeuken@lic.leidenuniv.nl

Authors

Rosa Catania − *Astbury Centre of Structural Molecular Biology and School of Biomedical Sciences, University of Leeds, Leeds LS2 9JT, U.K.;* orcid.org/0000-0002-4717-808X

Jonathan Machin − *Astbury Centre of Structural Molecular Biology and School of Biomedical Sciences, University of Leeds, Leeds LS2 9JT, U.K.*

Michael Rappolt − *School of Food Science and Nutrition, University of Leeds, Leeds LS2 9JT, U.K.;* orcid.org/0000-0001-9942-3035

Stephen P. Muench − *Astbury Centre of Structural Molecular Biology and School of Biomedical Sciences, University of Leeds, Leeds LS2 9JT, U.K.*

Complete contact information is available at: https://pubs.acs.org/10.1021/acs.macromol.2c00326

Notes

The authors declare no competing financial interest.

■ ACKNOWLEDGMENTS

We gratefully thank Dr Huijie Zhang for the assistance provided with the setting up of electrochemistry and fluorescence measurements, and Dr Rashmi Seneviratne for training and support on making and characterizing hybrid vesicles. This work was funded by the Biotechnology and Biological Sciences Research Council (BBSRC), grant number BB/T000546/1, and the Wellcome Trust, grant number 222373/Z/21/Z.

■ REFERENCES

(1) Cintas, P. Chasing Synthetic Life: A Tale of Forms, Chemical Fossils, and Biomorphs. *Angew. Chem. Int. Ed.* **2020**, *132*, 7364−7372.

(2) Elani, Y. Interfacing Living and Synthetic Cells as an Emerging Frontier in Synthetic Biology. *Angew. Chem. Int. Ed.* **2021**, *60* (11), 5602−5611.

(3) Wang, G.; Castiglione, K. Light-Driven Biocatalysis in Liposomes and Polymersomes: Where Are We Now ? *Catalysts* **2019**, *9* (12), 1−25.

(4) Pannwitz, A.; Klein, D. M.; Rodrıguez-Jimenez, S.; Casadevall, C.; Song, H.; Reisner, E.; Hammarstro, L.; Bonnet, S. Roadmap towards Solar Fuel Synthesis at the Water Interface of Liposome Membranes. *Chem. Soc. Rev.* **2021**, *50*, 4833−4855.

(5) Yin, H.; Flynn, A. D. Drugging Membrane Protein Interactions Hang. *Annu. Rev. Biomed. Eng.* **2016**, *18*, 51−76.

(6) van der Pol, L.; Stork, M.; van der Ley, P. Outer Membrane Vesicles as Platform Vaccine Technology. *Biotechnol. J.* **2015**, *10* (11), 1689−1706.

(7) Alvarez-Malmagro, J.; García-Molina, G.; De Lacey, A. L. Electrochemical Biosensors Based on Membrane-Bound Enzymes in Biomimetic Configurations. *Sensors* **2020**, *20* (12), 1−17.

(8) Zhang, H.; Catania, R.; Jeuken, L. J. C. Membrane Protein Modified Electrodes in Bioelectrocatalysis. *Catalysts* **2020**, *10* (12), 1−29.

(9) Rideau, E.; Dimova, R.; Schwille, P.; Wurm, F. R.; Landfester, K. Liposomes and Polymersomes: A Comparative Review towards Cell Mimicking. *Chem. Soc. Rev.* **2018**, *47* (23), 8572−8610.

(10) Skrzypek, R.; Iqbal, S.; Callaghan, R. Methods of Reconstitution to Investigate Membrane Protein Function. *Methods* **2018**, *147*, 126−141.

(11) Amati, A. M.; Graf, S.; Deutschmann, S.; Dolder, N.; Von Ballmoos, C. Current Problems and Future Avenues in Proteoliposome Research. *Biochem. Soc. Trans.* **2020**, *48* (4), 1473−1492.

(12) Discher, D. E.; Eisenberg, A. Polymer Vesicles. *Science* **2002**, *967* (5583), 967−973.

(13) Palivan, C. G.; Goers, R.; Najer, A.; Zhang, X.; Car, A.; Meier, W. Bioinspired Polymer Vesicles and Membranes for Biological and Medical Applications. *Chem. Soc. Rev.* **2016**, *45* (2), 377−411.

(14) LoPresti, C.; Lomas, H.; Massignani, M.; Smart, T.; Battaglia, G. Polymersomes: Nature Inspired Nanometer Sized Compartments. *J. Mater. Chem.* **2009**, *19* (22), 3576−3590.

(15) Beales, P. A.; Khan, S.; Muench, S. P.; Jeuken, L. J. C. Durable Vesicles for Reconstitution of Membrane Proteins in Biotechnology. *Biochem. Soc. Trans.* **2017**, *45* (1), 15−26.
(16) Khan, S.; Li, M.; Muench, S. P.; Jeuken, L. J. C.; Beales, P. A. Durable Proteo-Hybrid Vesicles for the Extended Functional Lifetime of Membrane Proteins in Bionanotechnology. *Chem. Commun.* **2016**, *52* (73), 11020−11023.
(17) Paxton, W. F.; McAninch, P. T.; Achyuthan, K. E.; Shin, S. H. R.; Monteith, H. L. Monitoring and Modulating Ion Traffic in Hybrid Lipid/Polymer Vesicles. *Colloids Surf., B* **2017**, *159*, 268−276.
(18) Jacobs, M. L.; Boyd, M. A.; Kamat, N. P. Diblock Copolymers Enhance Folding of a Mechanosensitive Membrane Protein during Cell-Free Expression. *Proc. Natl. Acad. Sci. U. S. A.* **2019**, *116* (10), 4031−4036.
(19) Marušič, N.; Otrin, L.; Zhao, Z.; Lira, R. B.; Kyrilis, F. L.; Hamdi, F.; Kastritis, P. L.; Vidaković-Koch, T.; Ivanov, I.; Sundmacher, K.; Dimova, R. Constructing Artificial Respiratory Chain in Polymer Compartments: Insights into the Interplay between Bo3 Oxidase and the Membrane. *Proc. Natl. Acad. Sci. U. S. A.* **2020**, *117* (26), 15006−15017.
(20) Rottet, S.; Iqbal, S.; Beales, P. A.; Lin, A.; Lee, J.; Rug, M.; Scott, C.; Callaghan, R. Characterisation of Hybrid Polymersome Vesicles Containing the Efflux Pumps NaAtm1 or P-Glycoprotein. *Polymers* **2020**, *12* (5), 1049.
(21) Schulz, M.; Binder, W. H. Mixed Hybrid Lipid/Polymer Vesicles as a Novel Membrane Platform. *Macromol. Rapid Commun.* **2015**, *23* (36), 2031−2041.
(22) Le Meins, J. F.; Schatz, C.; Lecommandoux, S.; Sandre, O. Hybrid Polymer/Lipid Vesicles: State of the Art and Future Perspectives. *Mater. Today* **2013**, *16* (10), 397−402.
(23) Seneviratne, R.; Khan, S.; Moscrop, E.; Rappolt, M.; Muench, S. P.; Jeuken, L. J. C.; Beales, P. A. A Reconstitution Method for Integral Membrane Proteins in Hybrid Lipid-Polymer Vesicles for Enhanced Functional Durability. *Methods* **2018**, *147*, 142−149.
(24) Moraes, I.; Evans, G.; Sanchez-Weatherby, J.; Newstead, S.; Shaw Stewart, P. D. Membrane Protein Structure Determination — The next Generation. *Biochim. Biophys. Acta - Biomembranes* **2014**, *1838* (1), 78−87.
(25) Seddon, A. M.; Curnow, P.; Booth, P. J. Membrane Proteins, Lipids and Detergents : Not Just a Soap Opera. *Biochim. Biophys. Acta* **2004**, *1666* (1−2), 105−117.
(26) Palsdottir, H.; Hunte, C. Lipids in Membrane Protein Structures. *Biochim. Biophys. Acta* **2004**, *1666* (1−2), 2−18.
(27) Privé, G. G. Detergents for the Stabilization and Crystallization of Membrane Proteins. *Methods* **2007**, *41* (4), 388−397.
(28) Postis, V. L. G.; Deacon, S. E.; Roach, P. C. J.; Wright, G. S. A.; Xia, X.; Wright, G. S. A.; Xia, X.; Ingram, J. C.; Hadden, J. M.; Peter, J.; Henderson, F.; Phillips, S. E. V; Roach, P. C. J.; Mcpherson, M. J.; Baldwin, S. A. A High-Throughput Assay of Membrane Protein Stability. *Mol. Membr. Biol.* **2008**, *25* (8), 617−624.
(29) Garcia-Horsman, A. J.; Barquera, B.; Rumbley, J.; Ma, J.; Gennis, R. B. The Superfamily of Heme-Copper Respiratory Oxidases. *J. Bacteriol.* **1994**, *176* (18), 5587−5600.
(30) Lim, S. K.; de Hoog, H.-P.; Parikh, A. N.; Nallani, M.; Liedberg, B. Hybrid, Nanoscale Phospholipid/Block Copolymer Vesicles. *Polymers* **2013**, *5* (3), 1102−1114.
(31) Li, J.; Han, L.; Vallese, F.; Ding, Z.; Choi, S. K.; Hong, S.; Luo, Y.; Liu, B.; Chan, C. K.; Tajkhorshid, E.; Zhu, J.; Clarke, O.; Zhang, K.; Gennis, R. Cryo-EM Structures of Escherichia Coli Cytochrome Bo 3 Reveal Bound Phospholipids and Ubiquinone-8 in a Dynamic Substrate Binding Site. *Proc. Natl. Acad. Sci. U. S. A.* **2021**, *118* (34), e2106750118.
(32) Lee, S. C.; Knowles, T. J.; Postis, V. L. G.; Jamshad, M.; Parslow, R. A.; Lin, Y.; Goldman, A.; Sridhar, P.; Overduin, M.; Muench, S. P.; Dafforn, T. R. A Method for Detergent-Free Isolation of Membrane Proteins in Their Local Lipid Environment. *Nat. Protoc.* **2016**, *11* (7), 1149−1162.
(33) Knowles, T. J.; Finka, R.; Smith, C.; Lin, Y.; Dafforn, T.; Overduin, M. Membrane Proteins Solubilized Intact in Lipid Containing Nanoparticles Bounded by Styrene Maleic Acid Copolymer. *J. Am. Chem. Soc.* **2009**, *131* (22), 7484−7485.
(34) Jamshad, M.; Charlton, J.; Lin, Y.; Routledge, S. J.; Bawa, Z.; Knowles, T. J.; Overduin, M.; Dekker, N.; Dafforn, T. R.; Bill, R. M.; Poyner, D. R.; Wheatley, M. G-Protein Coupled Receptor Solubilization and Purification for Biophysical Analysis and Functional Studies, in the Total Absence of Detergent. *Biosci. Rep.* **2015**, *35* (2), e00188.
(35) Tonge, S. R.; Tighe, B. J. Responsive Hydrophobically Associating Polymers : A Review of Structure and Properties. *Adv. Drug Delivery Rev.* **2001**, *53* (1), 109−122.
(36) Esmaili, M.; Overduin, M. Membrane Biology Visualized in Nanometer-Sized Discs Formed by Styrene Maleic Acid Polymers. *Biochim. Biophys. Acta - Biomembranes* **2018**, *1860* (2), 257−263.
(37) Orekhov, P. S.; Bozdaganyan, M. E.; Voskoboynikova, N.; Mulkidjanian, A. Y.; Steinhoff, H.-J.; Shaitan, K. V. Styrene/Maleic Acid Copolymers Form SMALPs by Pulling Lipid Patches out of the Lipid Bilayer. *Langmuir* **2019**, *35* (10), 3748−3758.
(38) Hesketh, S. J.; Klebl, D. P.; Higgins, A. J.; Thomsen, M.; Pickles, I. B.; Sobott, F.; Sivaprasadarao, A.; Postis, V. L. G.; Muench, S. P. Styrene Maleic-Acid Lipid Particles (SMALPs) into Detergent or Amphipols: An Exchange Protocol for Membrane Protein Characterisation. *Biochim. Biophys. Acta - Biomembranes* **2020**, *1862* (5), 183192.
(39) Pollock, N. L.; Lee, S. C.; Patel, J. H.; Gulamhussein, A. A.; Rothnie, A. J. Structure and Function of Membrane Proteins Encapsulated in a Polymer-Bound Lipid Bilayer. *Biochim. Biophys. Acta - Biomembranes* **2018**, *1860* (4), 809−817.
(40) Dörr, J. M.; Koorengevel, M. C.; Schäfer, M.; Prokofyev, A. V.; Scheidelaar, S.; van der Cruijesn, E. A. W.; Dafforn, T. R.; Baldus, M.; Killian, A. J. Detergent-Free Isolation, Characterization, and Functional Reconstitution of a Tetrameric K+ Channel: The Power of Native Nanodiscs. *Proc. Natl. Acad. Sci. U. S. A.* **2014**, *111* (52), 18607−18612.
(41) Smirnova, I. A.; Ädelroth, P.; Brzezinski, P. Extraction and Liposome Reconstitution of Membrane Proteins with Their Native Lipids without the Use of Detergents. *Sci. Rep.* **2018**, *8* (1), 14950.
(42) Dutta, D.; Esmaili, M.; Overduin, M.; Fliegel, L. Expression and Detergent Free Purification and Reconstitution of the Plant Plasma Membrane Na+/H+ Antiporter SOS1 Overexpressed in Pichia Pastoris. *Biochim. Biophys. Acta - Biomembranes* **2020**, *1862* (3), 183111.
(43) Oluwole, A. O.; Danielczak, B.; Meister, A.; Babalola, J. O.; Vargas, C.; Keller, S. Solubilization of Membrane Proteins into Functional Lipid-Bilayer Nanodiscs Using a Diisobutylene/Maleic Acid Copolymer. *Angew. Chem. Int. Ed.* **2017**, *56* (7), 1919−1924.
(44) Gulamhussein, A. A.; Uddin, R.; Tighe, B. J.; Poyner, D. R.; Rothnie, A. J. A Comparison of SMA (Styrene Maleic Acid) and DIBMA (Di-Isobutylene Maleic Acid) for Membrane Protein Purification. *Biochim. Biophys. Acta - Biomembranes* **2020**, *1862* (7), 183281.
(45) Barniol-Xicota, M.; Verhelst, S. H. L. Lipidomic and In-Gel Analysis of Maleic Acid Co-Polymer Nanodiscs Reveals Differences in Composition of Solubilized Membranes. *Commun. Biol.* **2021**, *4* (1), 218.
(46) Di Mauro, G. M.; La Rosa, C.; Condorelli, M.; Ramamoorthy, A. Benchmarks of SMA-Copolymer Derivatives and Nanodisc Integrity. *Langmuir* **2021**, *37* (10), 3113−3121.
(47) Hall, S. C. L.; Tognoloni, C.; Charlton, J.; Bragginton, É. C.; Rothnie, A. J.; Sridhar, P.; Wheatley, M.; Knowles, T. J.; Arnold, T.; Edler, K. J.; Dafforn, T. R. An Acid-Compatible Co-Polymer for the Solubilization of Membranes and Proteins into Lipid Bilayer-Containing Nanoparticles. *Nanoscale* **2018**, *10* (22), 10609−10619.
(48) Rumbley, J. N.; Nickels, E. F.; Gennis, R. B. One-Step Purification of Histidine-Tagged Cytochrome Bo3 from Escherichia Coli and Demonstration That Associated Quinone Is Not Required for the Structural Integrity of the Oxidase. *Biochim. Biophys. Acta - Protein Struct. Mol. Enzym.* **1997**, *1340* (1), 131−142.

https://doi.org/10.1021/acs.macromol.2c00326
Macromolecules XXXX, XXX, XXX−XXX

(49) Morrison, K. A.; Akram, A.; Mathews, A.; Khan, Z. A.; Patel, J. H.; Zhou, C.; Hardy, D. J.; Moore-kelly, C.; Patel, R.; Odiba, V.; Knowles, T. J.; Javed, M.-H.; Chmel, N. P.; Dafforn, T. R.; Rothnie, A. J. Membrane Protein Extraction and Purification Using Styrene − Maleic Acid (SMA) Copolymer: Effect of Variations in Polymer Structure. *Biochem. J.* **2016**, *473* (23), 4349−4360.
(50) Liu, Y.; Moura, E. C. C. M.; Dörr, J. M.; Scheidelaar, S.; Heger, H.; Egmond, M. R.; Killian, J. A.; Mohammadi, T.; Breukink, E. Bacillus Subtilis MraY in Detergent-Free System of Nanodiscs Wrapped by Styrene-Maleic Acid Copolymers. *PLoS One* **2018**, *13* (11), 1−18.
(51) Barniol-Xicota, M.; Verhelst, S. H. L. Stable and Functional Rhomboid Proteases in Lipid Nanodiscs by Using Diisobutylene/Maleic Acid Copolymers. *J. Am. Chem. Soc.* **2018**, *140* (44), 14557−14561.
(52) Li, M.; Jørgensen, S. K.; Mcmillan, D. G. G.; Krzemiński, Ł. K.; Daskalakis, N. N.; Partanen, R. H.; Tutkus, M.; Tuma, R.; Stamou, D.; Hatzakis, N. S.; Jeuken, L. J. C. Single Enzyme Experiments Reveal a Long-Lifetime Proton Leak State in a Heme-Copper Oxidase. *J. Am. Chem. Soc.* **2015**, *137* (51), 16055−16063.
(53) Mazurenko, I.; Hatzakis, N. S.; Jeuken, L. J. C. Single Liposome Measurements for the Study of Proton-Pumping Membrane Enzymes Using Electrochemistry and Fluorescent Microscopy. *J. Visualized Exp.* **2019**, No. 144, 1−11.
(54) Scheidelaar, S.; Koorengevel, M. C.; Pardo, J. D.; Meeldijk, J. D.; Breukink, E.; Killian, J. A. Molecular Model for the Solubilization of Membranes into Nanodisks by Styrene Maleic Acid Copolymers. *Biophys. J.* **2015**, *108* (2), 279−290.
(55) Kollmitzer, B.; Heftberger, P.; Rappolt, M.; Pabst, G. Monolayer Spontaneous Curvature of Raft-Forming Membrane Lipids. *Soft Matter* **2013**, *9* (45), 10877−10884.
(56) Dörr, J. M.; Scheidelaar, S.; Koorengevel, M. C.; Dominguez, J. J.; Schäfer, M.; van Walree, C. A.; Killian, J. A. The Styrene−Maleic Acid Copolymer: A Versatile Tool in Membrane Research. *Eur. Biophys. J.* **2016**, *45* (1), 3−21.
(57) Dominguez Pardo, J. J.; Dörr, J. M.; Iyer, A.; Cox, R. C.; Scheidelaar, S.; Koorengevel, M. C.; Subramaniam, V.; Killian, J. A. Solubilization of Lipids and Lipid Phases by the Styrene−Maleic Acid Copolymer. *Eur. Biophys. J.* **2017**, *46* (1), 91−101.
(58) Seneviratne, R.; Catania, R.; Rappolt, M.; Jeuken, L. J. C.; Beales, P. A. Membrane Mixing and Dynamics in Hybrid POPC/Poly(1,2-Butadiene- *Block* -Ethylene Oxide) (PBd-*b* -PEO) Lipid/Block Co-Polymer Giant Vesicles. *Soft Matter* **2022**, *18*, 1294.
(59) Bermudez, H.; Brannan, A. K.; Hammer, D. A.; Bates, F. S.; Discher, D. E. Molecular Weight Dependence of Polymersome Membrane Structure, Elasticity, and Stability. *Macromolecules* **2002**, *35* (21), 8203−8208.
(60) Nam, J.; Beales, P. A.; Vanderlick, T. K. Giant Phospholipid/Block Copolymer Hybrid Vesicles: Mixing Behavior and Domain Formation. *Langmuir* **2011**, *27* (1), 1−6.
(61) Rawicz, W.; Olbrich, K. C.; Mcintosh, T.; Needham, D.; Evans, E. Effect of Chain Length and Unsaturation on Elasticity of Lipid Bilayers. *Biophys. J.* **2000**, *79*, 328−339.

https://doi.org/10.1021/acs.macromol.2c00326
Macromolecules XXXX, XXX, XXX−XXX